Water Penetration in Glassy Polymers: Experiment and Theory

M. BEST, J. W. HALLEY,* B. JOHNSON, and J. L. VALLÉS

IBM Almaden Research Center, 650 Harry Road, San Jose, California 95120; School of Physics and Astronomy, University of Minnesota, Minneapolis, Minnesota 55455

SYNOPSIS

We describe the design and implementation of a method based on infrared monitoring of the OD stretch mode which permits measurement of the diffusion profiles of water permeating glassy polymers for the first time. Results for several glassy polymers are compared with a theory of trapping diffusion which leads to a nonlinear diffusion problem in which the trapped water penetrates the polymer as a sharp front if there is a large amount of trapping. In the case of two of the polymers studied, the trapping model describes the data, very well (much better than a simple diffusion model) and permits determination of parameters related to the free volume and the residence time of the water on traps in the model. © 1993 John Wiley & Sons, Inc.

INTRODUCTION

Water penetration of glassy polymers is a persistent problem in various industrial contexts. In the work reported here, we sought to understand the phenomenon better by a cooperative program of experiment and theory. In the experiments, water penetrating glassy polymer films was detected by use of infrared absorption studies of D_2O. In Figure 1 we show some diffusion profiles obtained with this technique for a variety of glassy polymers. Some profiles are clearly diffusionlike, whereas, in other cases, a more complicated penetration process is taking place.

The most commonly used existing theoretical models to describe the diffusion of water into polymers are versions of the dual-mode diffusion model[1,2] in which the trapping of water by the polymer plays a central role. We have addressed the question of the chemical identity of the traps in earlier theoretical work,[3] where we established that the trapping sites are likely to be alcohol groups, in agreement with earlier experimental work[4] on branched polyethylene. Elsewhere we have shown[5] some important consequences of the dual mode diffusion model (with trapping but without swelling of the polymer): Trapping results in a density profile of trapped water which is frontlike rather than being of diffusive form. Here we submit this theoretical conclusion to experimental check by the new infrared methods using heavy water. The next section summarizes the experimental method and results. The third section describes the model. Finally, we compare theory and experiment and present a discussion.

EXPERIMENTAL

Preliminary stability data were obtained for eight commercially available, optically clear adhesives. Several of the adhesives were one part, UV-curable, another was a siloxane epoxy that has two components and requires a cure at 120°C, and some were two component epoxies that cure at room temperature. The adhesives were chosen because of reported good adhesion to both glass and metal, thermal stability, mechanical properties, and an index of refraction near 1.5, which matches that of glass. They were either cured with UV light, or were cured after mixing at room temperature. Thermal gravimetric analysis (TGA) on the cured materials showed thermal stability to at least 150°C. We per-

* To whom correspondence should be addressed.

Journal of Applied Polymer Science, Vol. 48, 319–334 (1993)
 CCC 0021-8995/93/020319-16

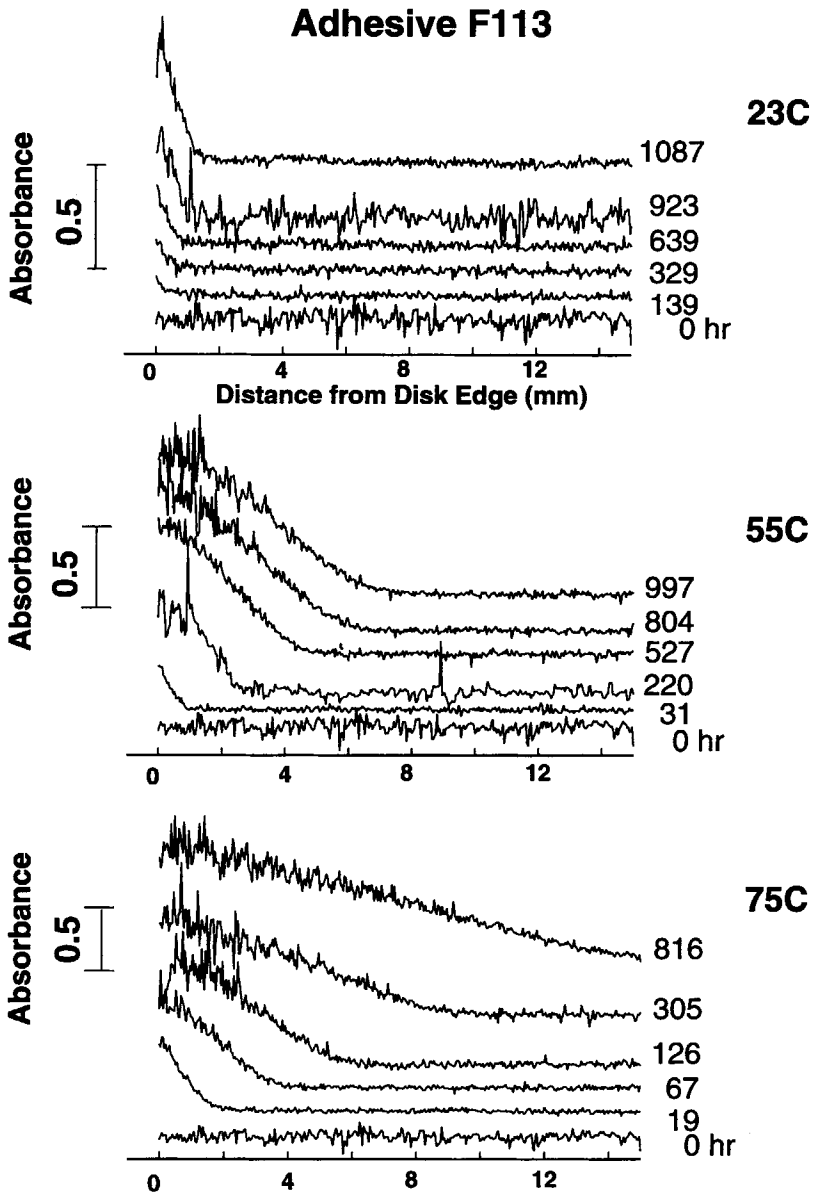

Figure 1 Absorbance data for F113.

formed standard[6] aging and temperature humidity (T/H) cycling tests on samples of all eight adhesives. Two of the adhesives changed color or delaminated under these tests. No further experiments were done with these two adhesives. New samples (which had not undergone aging or T/H cycling) were made for studying water adsorption in the remaining six adhesives. These six adhesives are listed in Table I together with supplier information, description of the adhesives, and the cure. Table II summarizes some of the mechanical data and properties of the adhesives.

The six transparent adhesives listed in Tables I and II were used to make a disk structure consisting of Glass–ZrO_2–adhesive–ZrO_2–glass. The 5-$\frac{1}{4}$ in. chemically hardened glass substrates were sputtered with 900 Å of ZrO_2. Since all these adhesives have a typical viscosity less than 300 cP at room temperature, just the weight of the top glass was enough to form thin bond lines (of approximately 20 μm). The glued disk structures were cut into eight coupons with a diamond saw. The coupons were submerged in D_2O at 23, 55, and 75°C for up to 1000 h. The D_2O was replaced with fresh D_2O every 4–5 days

Table I Adhesives with Good Thermal and Moisture Stability

Name	Manufacturer	Cure	Composition
Trabond TB2115	Tra-Con	RT cure, 24 h	Resin: bis-A epichlorohydrin epoxide reaction product Hardner: aliphatic polyamine mixture
Trabond F110	Tra-Con	RT cure, 24 h	Resin: as above Hardner: aliphatic alkylamine mixture
Trabond F113	Tra-Con	RT cure, 24 h	Resin: as above Hardner: aliphatic polyamine mixture
SILEP	IBM Research	120°C for 1.5 h	Siloxane + epoxy
NOA61	Norland	UV cure	Polyene, polythiol, initiators
NOA121	Norland	UV cure, 10 min at 125°C	Urethane polymer with reactive end groups, multifunctional mercaptan ester, initiators and stabilizers

Table II Summary of Adhesive Properties

NOA61	Specific gravity	1.29
	Refractive index	1.527
	TCE	22×10^{-6}
	T_g	23–25°C
	Operating temp	−80–90°C
	H_2O absorption	0.16%
NOA121	Specific gravity	1.29
	Refractive index	1.56
	TCE	225×10^{-6}
	T_g	35–40°C
	Operating temp	−60–150°C
	H_2O absorption	0.16%
TB F110	Specific gravity	1.16
	Refractive index	1.54
	TCE	60×10^{-6}
	T_g	100–110°C
	Operating temp	−60–130°C
	H_2O absorption	0.1%
TB F113	Specific gravity	1.22
	Refractive index	1.55
	TCE	55×10^{-6}
	T_g	90–100°C
	Operating temp	−60–100°C
	H_2O absorption	0.2%
TB 2115	Specific gravity	1.22
	Refractive index	1.55
	TCE	55×10^{-6}
	T_g	40–50°C
	Operating temp	−60–110°C
	H_2O absorption	0.3%
Siloxane epoxy	Refractive index	1.55
	T_g	−120°C, 15–20°C
	H_2O absorption	0.05%

to assure that the exchange of D_2O with water in the air did not significantly dilute the D_2O. Coupons were removed after various times of exposure and wiped off with a dry cloth, and the diffusion profile of the D_2O into the polymer was measured by monitoring the intensity of the OD stretch mode infrared absorption peak at 2550 cm^{-1} as a function of position in the coupon. For this purpose, a Perkin Elmer 983 infrared spectrometer set in time drive mode was used. In time drive mode, the peak intensity was measured each second while the coupon was moved across the infrared beam at 0.04 mm/s. A circular aperture of 1 mm diameter was put between the sample and the detector so that reported intensities are averages over such a circular region. An attenuator was placed in front of the reference beam to bring the absorbance onto scale.

Each time the coupon was removed, the absorbance was measured at a total of 400 spatial points. This measurement took a total time of 400 s (1 point/s). The last 50 points of the scan were discarded because the translation stage may be nonlinear when it is close to maximum range. The 40 values of the absorbance preceding the last 50 points were averaged, and the resulting average was subtracted from the rest of the data under the assumption that a only negligible amount of D_2O penetrated to the last 40 points. Since the scan starts before the edge of the disk, there is a sudden jump in the absorbance as the disk edge comes into the IR beam. All values of the absorbance associated with spatial points outside this onset point are discarded and 14 more points are discarded due to the resolution of the experiment (0.04 mm/s × 14 = 0.56 mm, which is $\frac{1}{2}$ of the diaphragm spot size). The resulting starting point is then set to 0 distance, and each value after

that is multiplied by the scan rate (0.04 mm/s) to get the distance into the disk. Results for all six adhesives are shown in Figures 1–6. The experiment was not repeated, but infrared absorption spectra were obtained from scans across two different paths from the center of the coupon to the edge at each time and temperature. The infrared data for the two scans was very similar in each case, and the scan with lowest noise was selected for analysis.

THEORETICAL MODEL

The dual-mode transport model was recently reviewed and extended in Ref. 2, where it was pointed out that it can be derived as an approximation from a lattice model for diffusion in a nonhomogeneous medium. In this model the equilibrium concentration c of water in the system is taken to be of the form

$$c = c_D + c_H = k_D P + \frac{c'_H BP}{(1 + BP)}$$

where P is the partial pressure of water in gas phase and k_D, B, and c'_H are constants. The two terms are interpreted as "dissolved" and "adsorbed" water, hence the name dual-mode transport. Correspondingly, in the lattice model, the sites of the polymer

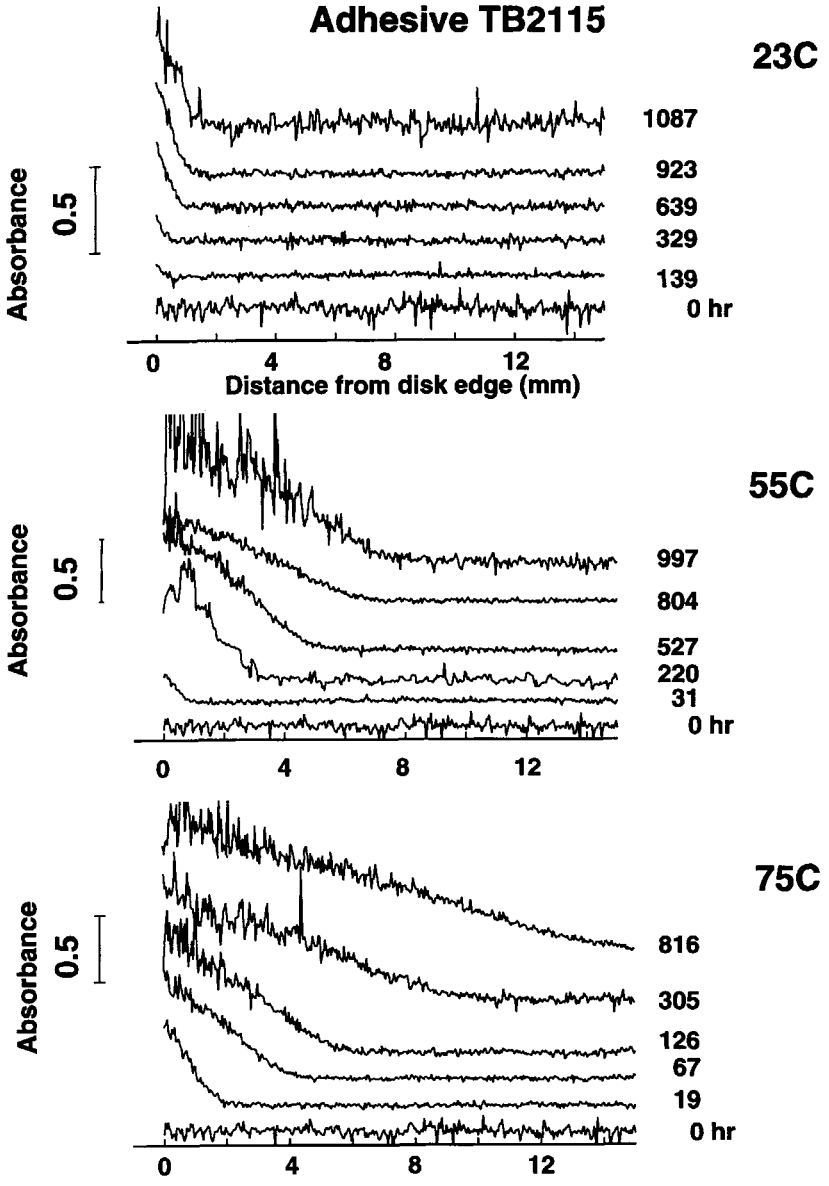

Figure 2 Absorbance data for TB2115.

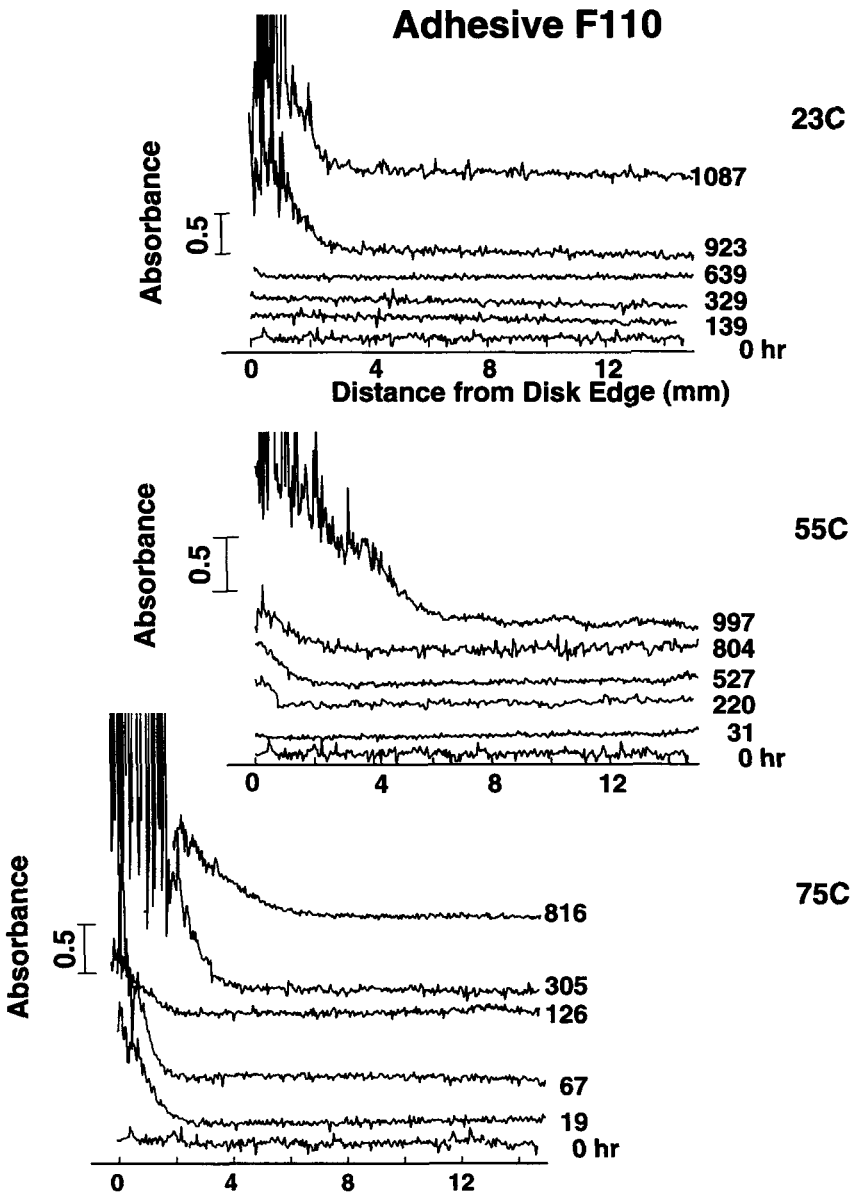

Figure 3 Absorbance data for F110.

matrix are of two types: those on which water can be "dissolved" (say white or w) and those sites in which the water can be "absorbed" (black or b). The model leading to Frederickson and Helfand's generalization of the dual-mode diffusion model is then a model for the diffusion of many particles on this disordered lattice according to the following rules: Particles hop from site to site according to a master equation, in such a way that there is not more than one particle at any site. There are three hopping rates in the problem, one for hopping from one w site to another, one for hopping between w and b sites, and one for hopping between b sites. Dynamical models of this type were first introduced by Kawasaki,[7] though they did not include the nonuniform background.

In earlier work,[5] we simulated this model on a lattice in the special case in which the particles hopping onto the trapping sites are trapped forever. We showed that this resulted in a sharp front of trapped particles and a diffusionlike profile of free particles. This is not hard to understand qualitatively: The first particles which diffuse into the medium are trapped by the trapping sites, and the following particles then diffuse normally. The total density is a combination of the sharp front of trapped particles

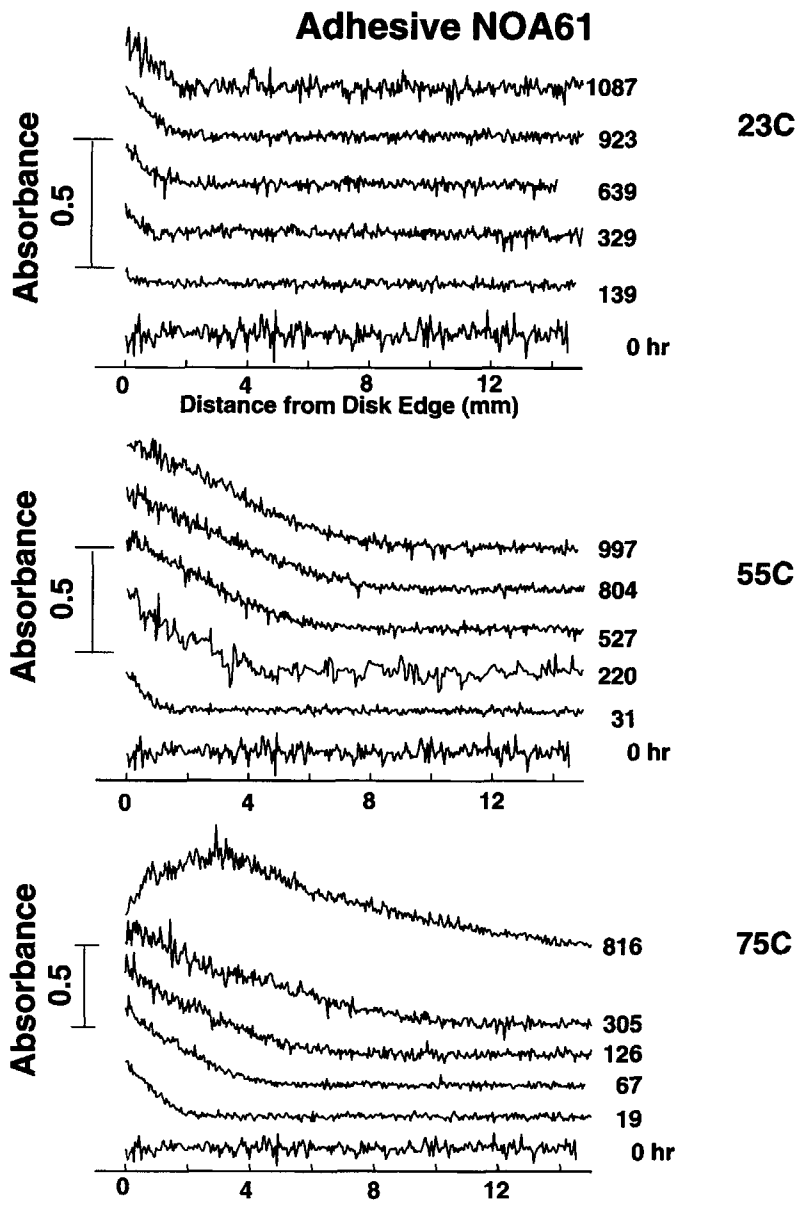

Figure 4 Absorbance data for NOA61.

and a diffusion profile behind it so that one gets a diffusion profile with a cutoff leading edge. A given particle "diffuses" freely through the region of bound particles (because all the trapping sites have been saturated and further trapping is impossible) and then becomes trapped at the "front." The model has interesting properties[5] associated with spatial fluctuations in the medium when the volume associated with the white (nontrapping) sites near the percolation value. If the volume fraction of nontrapping sites is far from percolation, however, the spatial fluctuations are not relevant to the behavior at long times and we can study a mean field version of the model (see Appendix A of Ref. 5).

In this mean field model we introduce variables b_i and w_i, which describe the average occupancy of black and white sites respectively in the ith $(d-1)$-dimensional plane parallel to the surface which contains the source s type sites. The master equations of the mean field model are then

$$\frac{dw_i}{dt} = W_{w\to w}(w_{i+1}(p - w_i) - w_i(p - w_{i+1}) - w_i(p - w_{i-1}) + w_{i-1}(p - w_i))$$

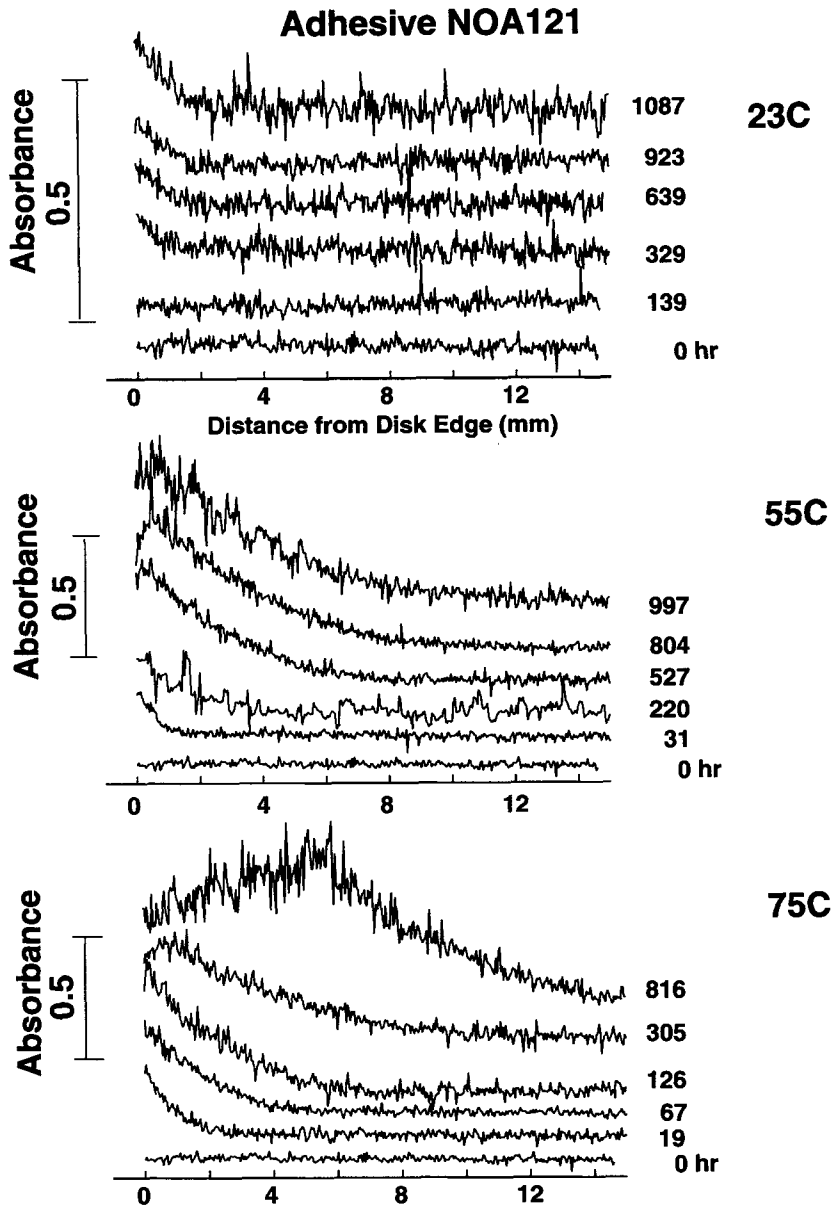

Figure 5 Absorbance data for NOA121.

$$- W_{w\to b} w_i (2 - 2p - b_{i+1} - b_{i-1}) + W_{b\to w}(b_{i+1} + b_{i-1})(p - w_i) \quad (1)$$

$$\frac{db_i}{dt} = W_{w\to b}(w_{i+1} + w_{i-1})(1 - p - b_i) - W_{b\to w} b_i (2p - w_{i+1} - w_{i-1}) \quad (2)$$

for $i > 1$ and

$$\frac{dw_1}{dt} = W_{w\to w}(w_2(p - w_1) - w_1(p - w_2)) - W_{w\to b} w_1 (1 - p - b_2) + W_{b\to w}(p - w_1) b_2 + W_{s\to w}(p - w_1) - W_{w\to s} w_1 \quad (3)$$

$$\frac{db_1}{dt} = W_{w\to b} w_2 (1 - p - b_1) - W_{b\to w} b_1 (p - w_2) + W_{s\to b}(1 - p - b_1) - W_{b\to s} b_1 \quad (4)$$

In these equations, the rates are constrained by the detailed balance condition requiring that at long times they cause the system to go to equilibrium. This gives the forms (Kawasaki dynamics)

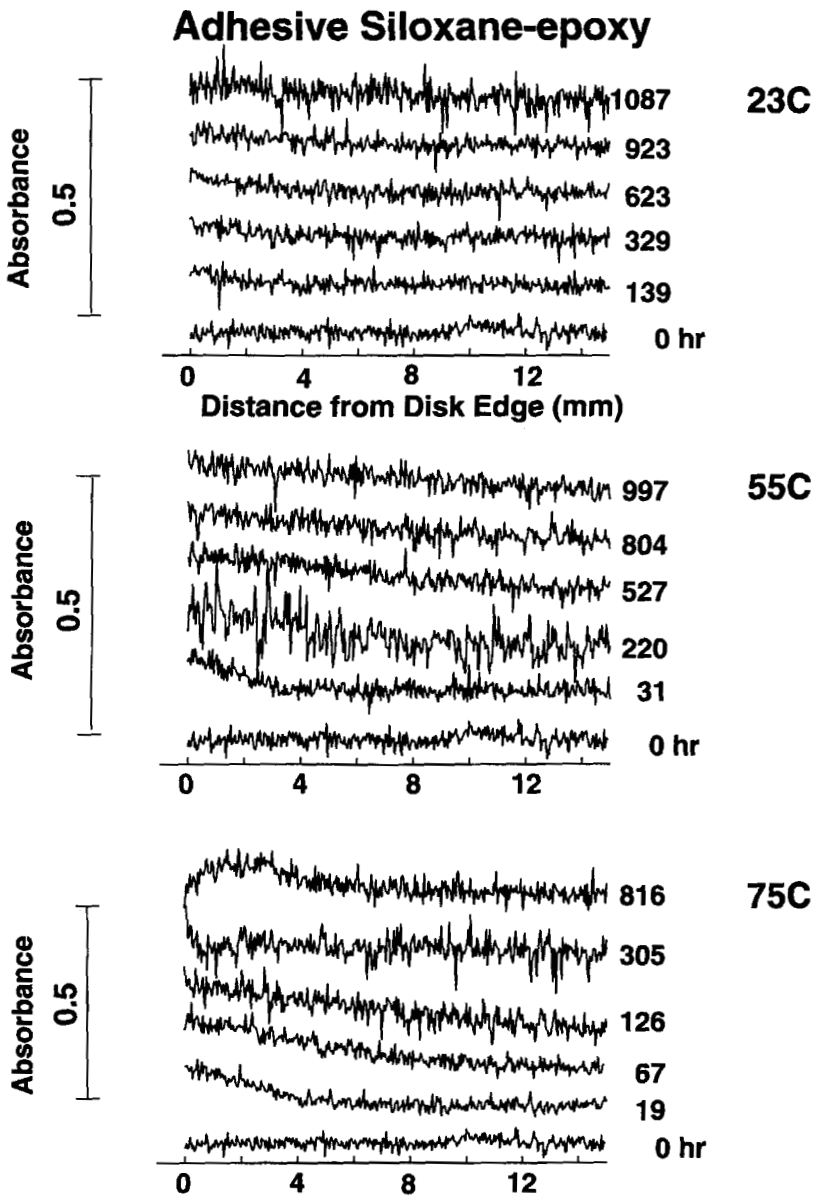

Figure 6 Absorbance data for siloxane epoxy.

$$W_{s\to w} = \frac{1}{\tau}\left(\frac{e^{\beta\phi/2}}{(e^{-\beta\phi/2} + e^{\beta\phi/2})}\right) \quad (5)$$

$$W_{w\to s} = e^{-\beta\phi} W_{s\to w} \quad (6)$$

$$W_{w\to b} = \frac{1}{\tau'}\left(\frac{e^{\beta\Delta/2}}{e^{-\beta\Delta/2} + e^{\beta\Delta/2})}\right) \quad (7)$$

$$W_{b\to w} = e^{-\beta\Delta} W_{w\to b} \quad (8)$$

$$W_{s\to b} = \frac{1}{\tau''}\left(\frac{e^{\beta(\phi+\Delta)/2}}{e^{-\beta(\phi+\Delta)/2} + e^{\beta(\phi+\Delta)/2})}\right) \quad (9)$$

$$W_{b\to s} = e^{-\beta(\phi+\Delta)} W_{s\to b} \quad (10)$$

$$W_{b\to b} = 0.0 \quad (11)$$

$$W_{w\to w} = 1/\tau_0 \quad (12)$$

This is quite a general formulation except that the possibility of the particles hopping from one b site to another is excluded. Though we did not use the full generality of this model in the calculation reported in Ref. 5, it will prove useful in applications to the interpretation of experiments reported here. β is the inverse temperature. The kinetic parameters $1/\tau_0$, $1/\tau$, $1/\tau'$, $1/\tau''$ are not known. The choice of

$\beta\phi$ controls the concentration of diffusant at the surface and will not affect the functional form of the diffusion profiles as long as the concentration is low enough so that self avoiding effects are negligible. We take $\beta\phi = 1$. For the same reason, the profile shapes will not be affected by the value of $1/\tau$ as long as saturation is not important and we take $1/\tau = 1/\tau_0$. The kinetic parameter $1/\tau_0$ sets the time scale, or equivalently, determines the diffusion coefficient in the absence of trapping. The kinetic parameter $1/\tau'$ controls the relative rates of the processes $w \rightarrow b$ relative to $w \rightarrow w$ at infinite temperature. As long as we are not seeking a full description of the temperature dependence, this relative rate can be varied at fixed temperature by varying $\beta\Delta$ and we take that approach here setting $1/\tau' = 1/\tau_0$. By a similar argument we take $1/\tau'' = 1/\tau_0$. The remaining parameters are $\beta\Delta$, which controls the relative rate at which diffusant leaves the "black" trapping sites and the white concentration p.

COMPARISON OF THE TRAPPING MODEL WITH THE EXPERIMENTS

A qualitative inspection of the data in Figures 1–6 shows that no measurable water absorption occurred in the siloxane adhesive, while the adhesives NOA61 and NOA121 showed nonmonotonic diffusant profiles at high temperatures and long times. Such nonmonotonicity cannot be explained by the theory of the preceding section. Accordingly, we focus attention here on the adhesives F113, TB2115, and F110.

The prediction of ordinary diffusion theory for this penetration problem is simply a profile of the form[8] $n(x, t) = n_0 \operatorname{erf} c(x/2\sqrt{(Dt)})$, where D is the diffusion constant. To compare the data for F113, TB2115, and F110 with this prediction, we first plot it for the three available temperatures ($T_1 = 23°C$, $T_2 = 55°C$ and $T_3 = 75°C$) as a function of $x/\sqrt{(Dt)}$ in which the relative values of D are chosen to make the data fall as nearly as possible on the same curve for all the times and for all three temperatures. The results are shown in Figures 7–15. The D values chosen are in the ratio $D(T_1) : D(T_2) : D(T_3) = 1 : 25 : 144$ for F113, $D(T_1) : D(T_2) : D(T_3) = 1 : 48 : 200$ for TB2115, and $D(T_1) : D(T_2) : D(T_3) = 1 : 1 : 12$ for F110. These values collapse the data for different temperatures and times quite well except at short times. The ratios of diffusion constants needed for F113 and TB2115 would correspond to an activated diffusion constant with an activation of energy of order 10,000 K. Though the physical origin of such a high activation energy is

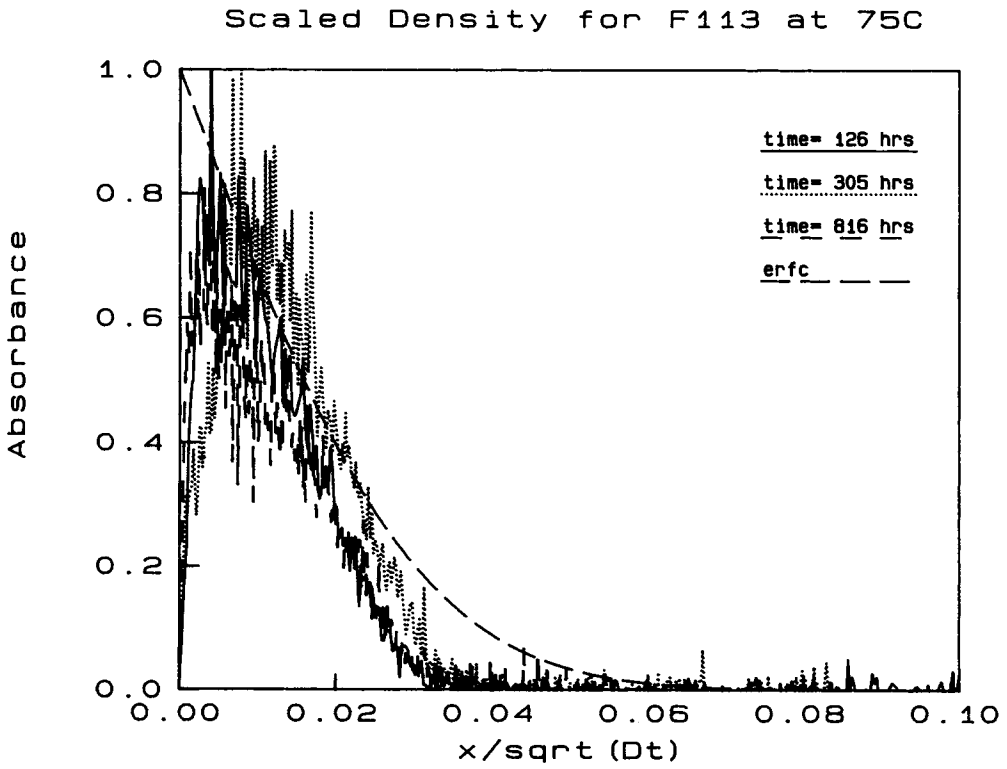

Figure 7 Scaled data for F113 at 75°C compared with diffusion equation prediction.

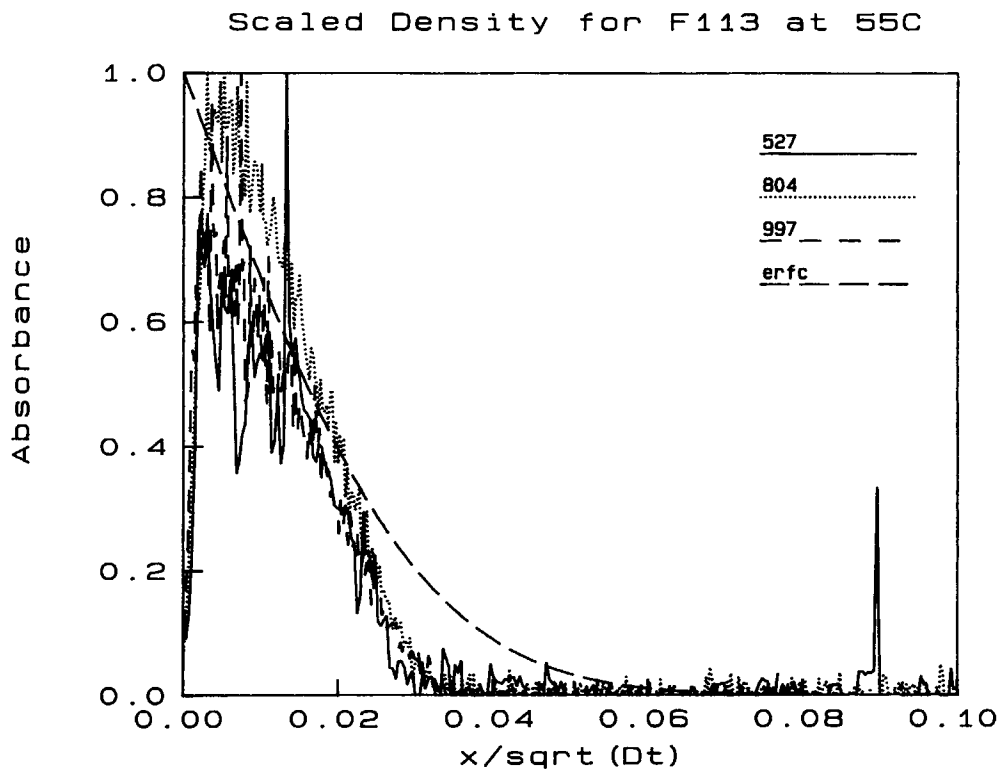

Figure 8 Scaled data for F113 at 55°C compared with diffusion equation prediction.

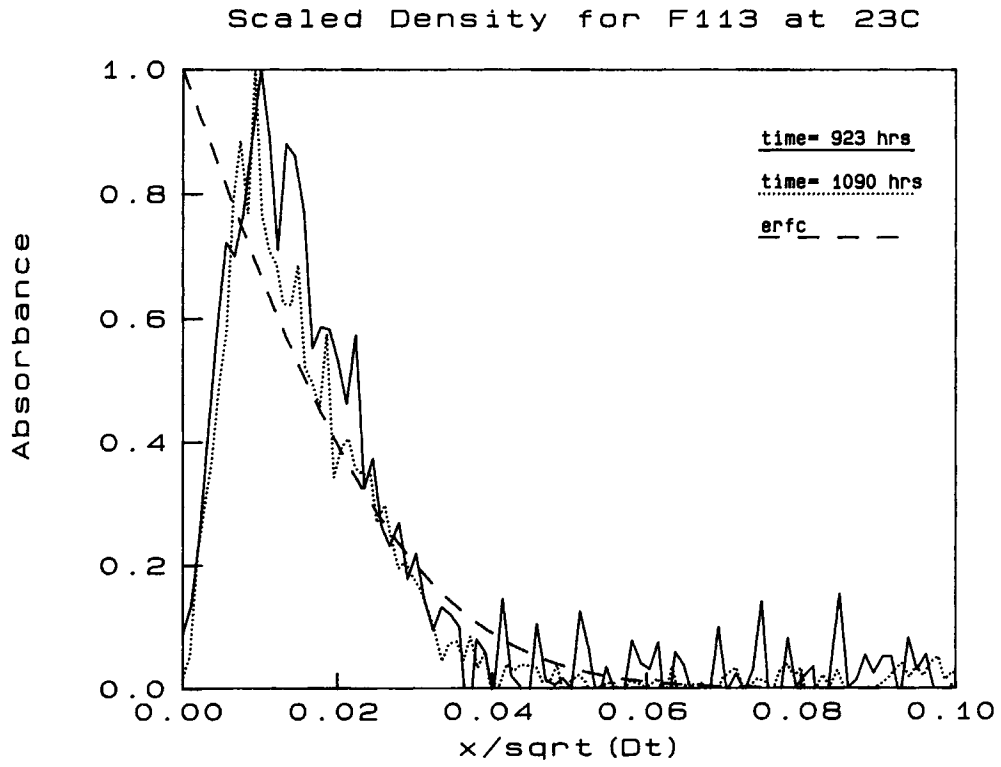

Figure 9 Scaled data for F113 at 23°C compared with diffusion equation prediction.

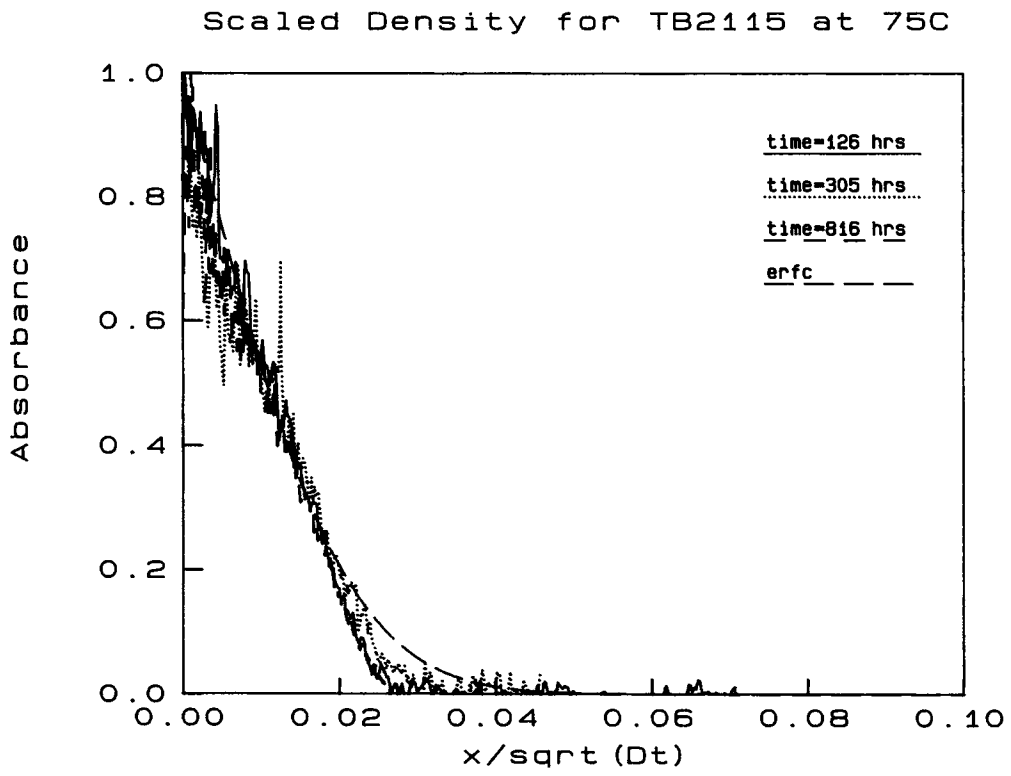

Figure 10 Scaled data for TB2115 at 75°C compared with diffusion equation prediction.

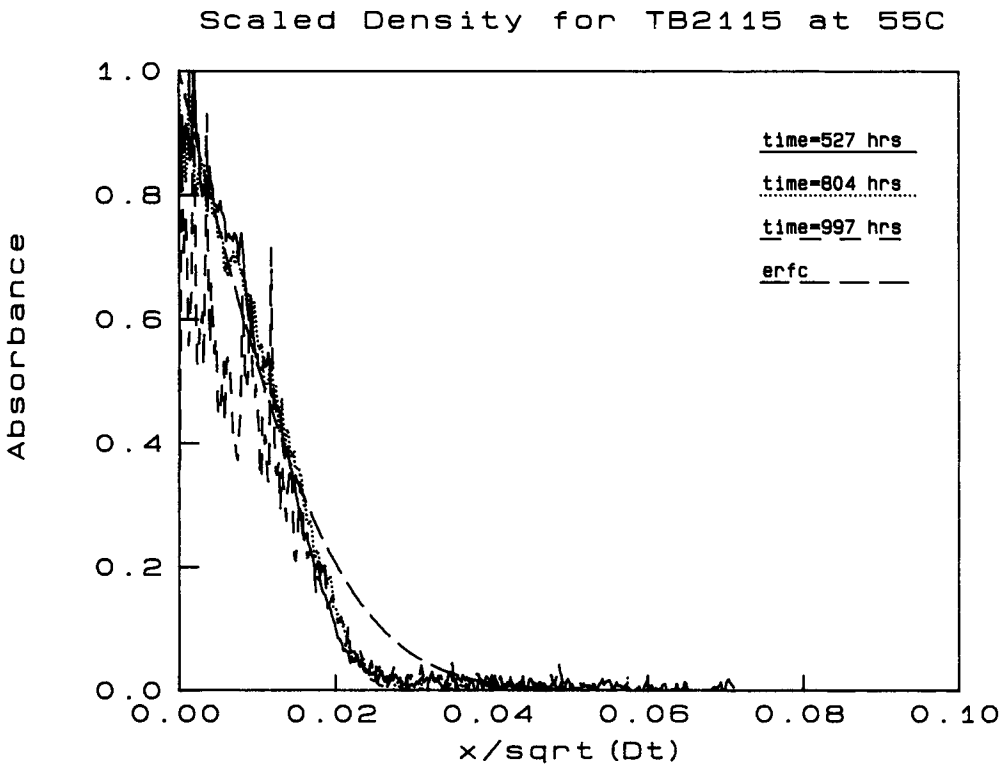

Figure 11 Scaled data for TB2115 at 55°C compared with diffusion equation prediction.

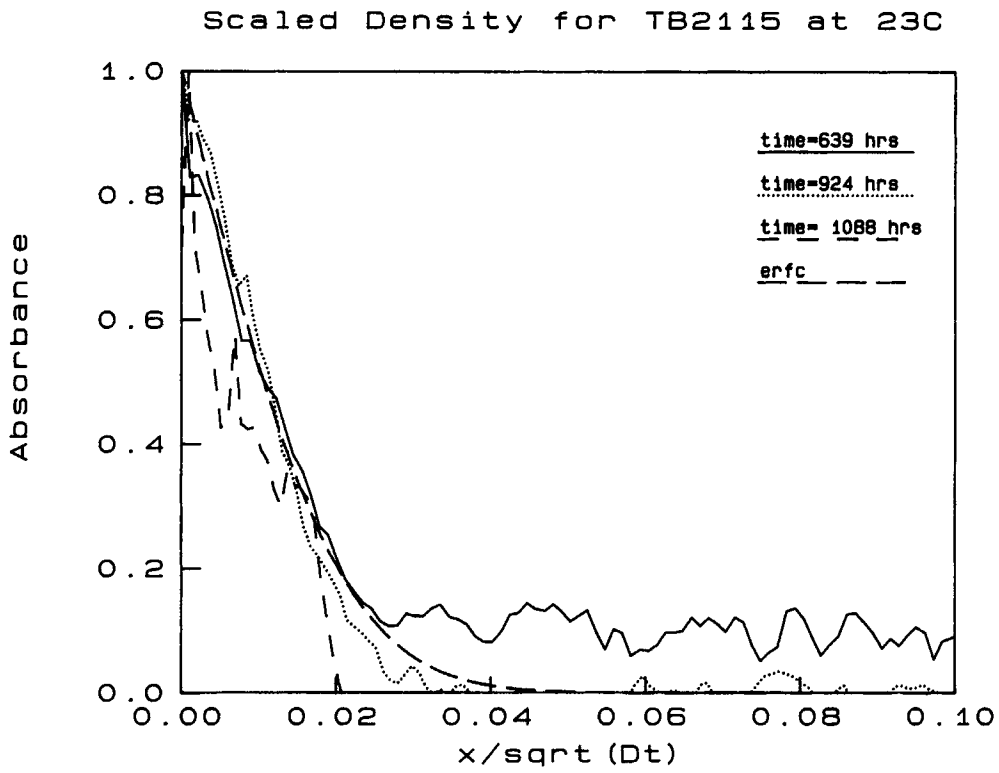

Figure 12 Scaled data for TB2115 at 23°C compared with diffusion equation prediction.

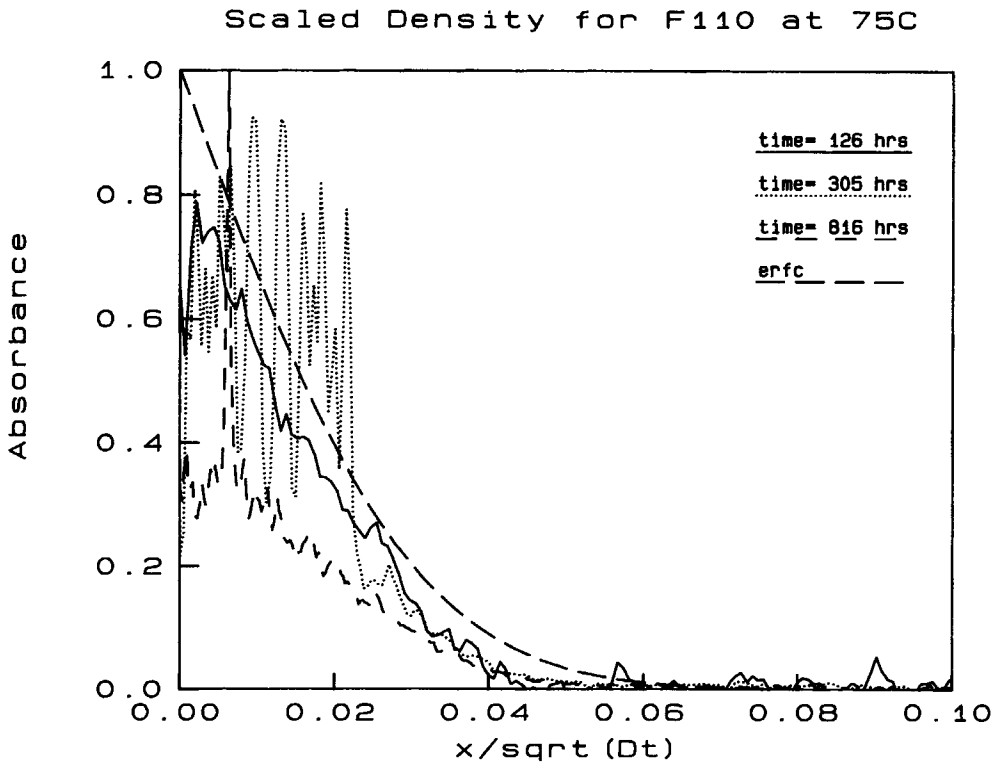

Figure 13 Scaled data for F110 at 75°C compared with diffusion equation prediction.

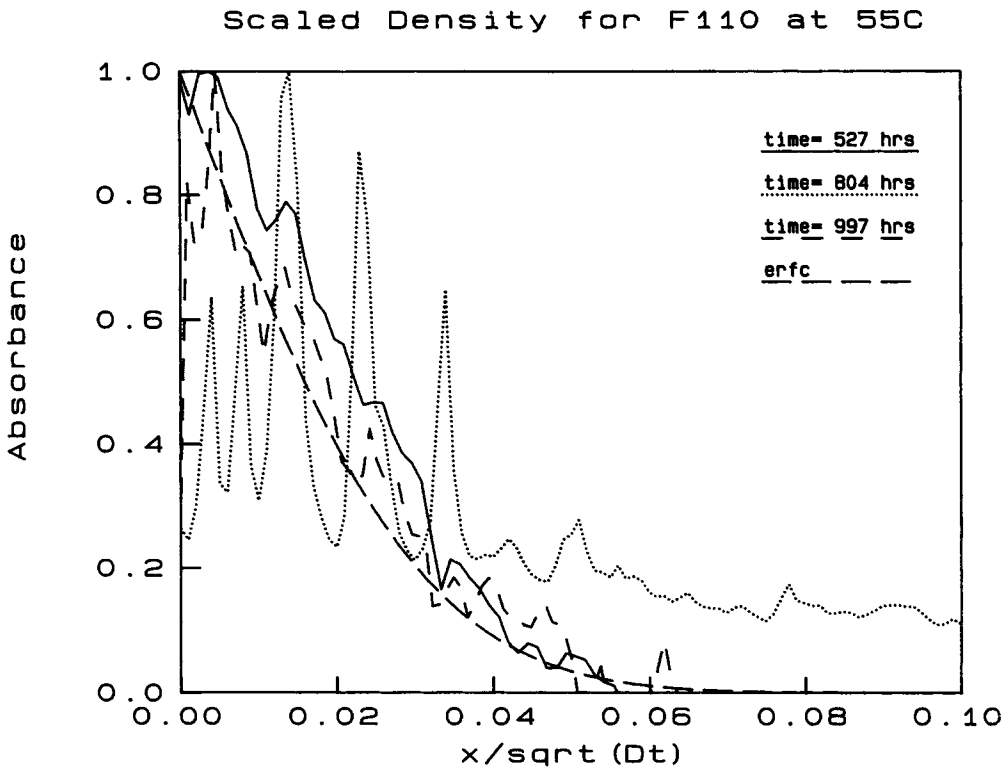

Figure 14 Scaled data for F110 at 55°C compared with diffusion equation prediction.

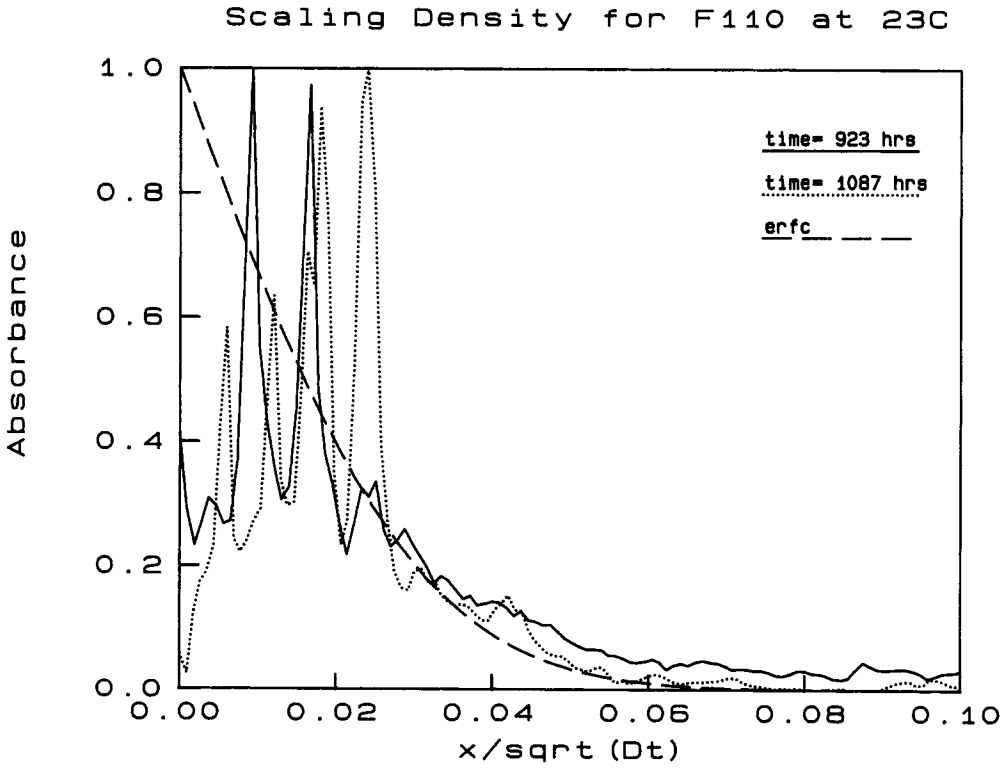

Figure 15 Scaled data for F110 at 23°C compared with diffusion equation prediction.

unclear, it is consistent with results on other glassy polymers.[9] To compare the scaled results with the diffusion prediction, we plot the complementary error function as the smooth curve in the same three figures. To make this comparison, we need to also select an absolute scale for the diffusion constant, and we have taken $D(T_1) = (1/900)$ mm^2/h for F113, $D(T_2) = (1/2000)$ mm^2/h for TB2115, and $D(T_2) = (1/900)$ mm^2/h for F110 in the figures. One sees that the data fit the diffusion reasonably well at intermediate distances, but, for F113 and TB2115, they fall below the diffusion prediction near the leading edge as qualitatively predicted by our models. (We have shown that the discrepancies with the diffusion model at short times are probably due to the finite size of the aperture in the infrared experiments.)

We showed above that the temperature dependence of the profiles for F110, F113, and TB2115 at intermediate distances can be understood within the context of a simple diffusion model. We next explore whether the discrepancies observed at larger distances in F113 and TB2115 can be understood by use of the trapping model described in the last section. To make this comparison, we use the data for F113 at 55°C and the data for TB2115 at 75°C. These temperatures were selected because data for the whole range of the diffusion profile was available for them. In view of the temperature scaling exhibited in Figures 7–12, we expect that a comparison at the other temperatures for these two adhesives would yield similar results. In Figures 16 and 17 we show a comparison between the data on adhesive F113 at 55°C and 804 h with two solutions of the eqs. (1)–(4) of the last section. In Figure 16 we have taken $\beta\Delta \gg 1$ as in Ref. 5 and then varied the diffusion constant to get a good fit in the intermediate time regime and, by varying p, to get the point at which the model prediction falls away from the diffusion equation prediction to match the experiment. One sees in Figure 16 that the model with $\beta\Delta \gg 1$ "overcorrects" the diffusion theory and predicts a sharper front than that observed in this experiment. By using a finite value of $\beta\Delta$, one introduces a finite lifetime for diffusant on the trapping sites. Then, as shown in Figure 17, one can get a very good fit to the experiment. In Figure 17, we took $p = 0.7$ and $\beta\Delta = 3.7$.

Using the same procedures we fitted the model to the dat on TB2115 at 55°C at 804 h with results

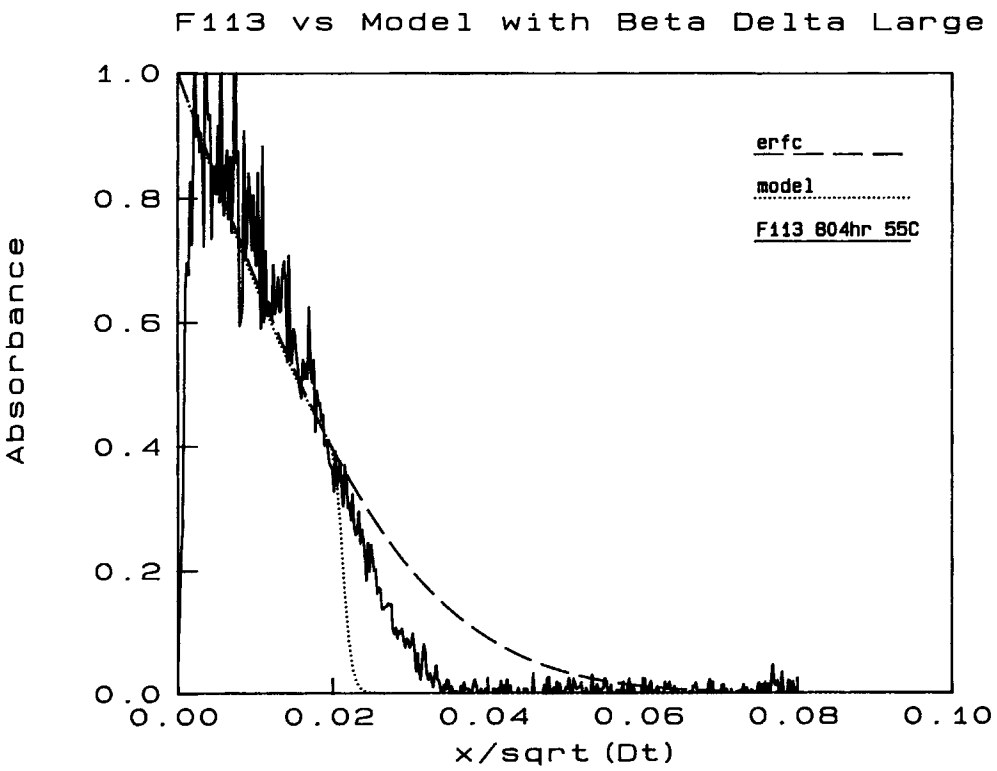

Figure 16 Comparison of F113 data at 55°C and 804 h with trapping model with infinite trapping time.

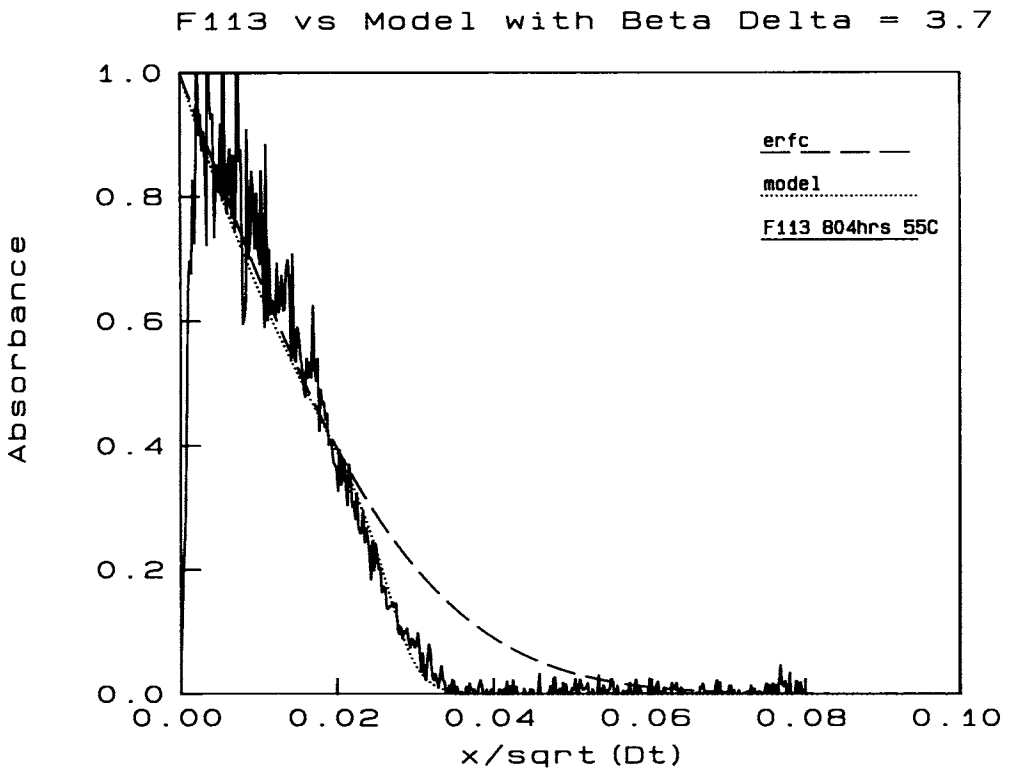

Figure 17 Comparison of F113 data at 55°C and 804 h with trapping model with finite trapping time.

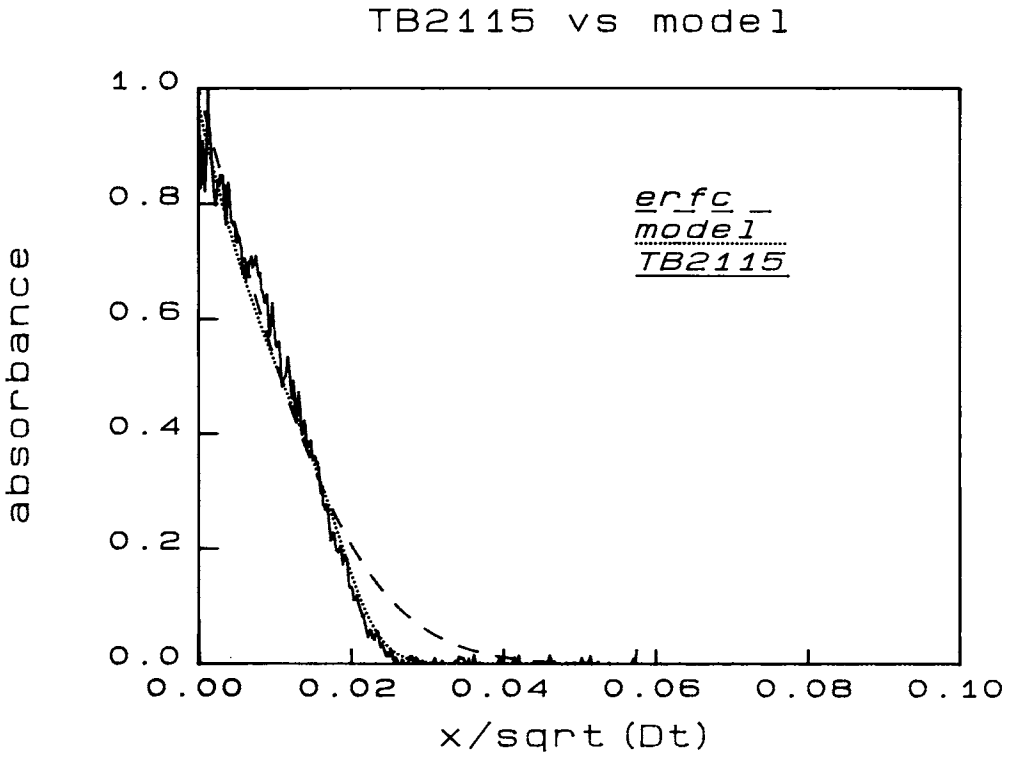

Figure 18 Comparison of TB2115 data at 55°C and 804 h with trapping model with finite trapping time.

shown in Figure 18. Here $p = 0.65$ and $\beta\Delta = 3.3$. In both Figures 17 and 18, the fit constrains the parameters to within a few percent of the values cited.

DISCUSSION, SUMMARY, AND FUTURE WORK

In this study we are concerned with the factors controlling the penetration of water into glassy polymers. Beyond standard diffusion theory, these factors are the trapping of the water by the polymer and the possible swelling response of the polymer to the diffusant. Here we have shown that a model taking account of trapping can account for the experimental results in the adhesives F113 and TB2115, if the model allows the diffusant to escape the trapping sites at a slow rate, whereas the data are clearly inconsistent with a simple diffusion model. The fits of the data to the model for these two adhesives are very good and strongly constrain the fitting parameters. The diffusant profiles in F110 were consistent with solutions to the diffusion equation without trapping, though the quality of the data was not very good in this case and less definitive conclusions can be drawn. The adhesives NOA121 and NOA61 showed nonmonotonic diffusant profiles at 816 h and 75°C. These cannot be explained by the trapping model and may be a manifestation of swelling. On the other hand, the fact that the anomalous behavior appeared only at one time and temperature might suggest an experimental artifact, and we cannot rule this out. The silane epoxy showed so little absorption that it was essentially not measurable by this technique. The activation energies required to account for the observed temperature dependence of the diffusion constants are surprising large, but are consistent with reports on other similar systems.[9]

We conclude that this technique for the study of diffusion of water into glassy polymer systems is a powerful one, capable of discriminating between linear and various nonlinear models of absorption in considerable detail.

This work was supported by a Supported University Research (SUR) Grant from the IBM Corporation and also from generous grants of supercomputer time from the Minnesota Supercomputer Institute (MSI). J. L. V. is also thankful to MSI for support as a research fellow at the Institute during the two years that he was at the University of Minnesota. J. W. H. is grateful to IBM for the award of the Paul Flory Sabbatical award in 1987, which allowed the initiation of this project during his stay at the Almaden Research Center. Jim Lyerla is thanked for continuous advice, encouragement, and support.

REFERENCES

1. R. Blahnik, *Prog. Org. Coat.*, **11,** 353 (1983).
2. G. H. Fredrickson and E. Helfand, *Macromolecules,* **18,** 2201 (1985).
3. J. L. Vallés and J. W. Halley, *J. Chem. Phys.*, **92,** 694 (1990).
4. D. W. McCall, D. C. Douglass, L. L. Blyer, G. E. Johnson, L. W. Jelinski, and H. E. Bair, *Macromolecules,* **17,** 1644 (1984).
5. J. W. Halley, B. Johnson, and J.-L. Vallés, *Phys. Rev. B,* **42,** 4383 (1990).
6. International Electrotechnical Commission Publication 68-2-38, 1974.
7. K. Kawasaki, *Phys. Rev.*, **145,** 225 (1966).
8. L. R. Ingersoll and O. J. Zobel, *An Introduction to the Mathematical Theory of Heat Conduction,* Atheneum Press, Boston, 1913, p. 78.
9. J. A. Barrie, in *Diffusion in Polymers,* J. Crank and G. S. Park, Eds., Academic, New York, 1968, Chap. 8.

Received January 6, 1992
Accepted July 7, 1992